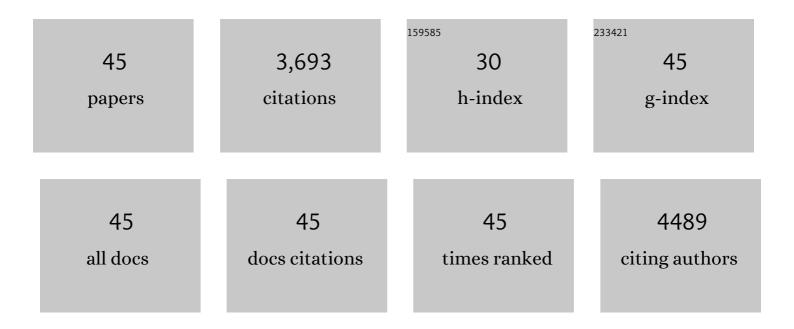
## Melissa Payer Sulprizio

List of Publications by Year in descending order

Source: https://exaly.com/author-pdf/9403387/publications.pdf Version: 2024-02-01



#	Article	IF	CITATIONS
1	Global mortality from outdoor fine particle pollution generated by fossil fuel combustion: Results from GEOS-Chem. Environmental Research, 2021, 195, 110754.	7.5	391
2	Why do models overestimate surface ozone in the Southeast United States?. Atmospheric Chemistry and Physics, 2016, 16, 13561-13577.	4.9	320
3	Public health impacts of the severe haze in Equatorial Asia in September–October 2015: demonstration of a new framework for informing fire management strategies to reduce downwind smoke exposure. Environmental Research Letters, 2016, 11, 094023.	5.2	249
4	Particulate air pollution from wildfires in the Western US under climate change. Climatic Change, 2016, 138, 655-666.	3.6	219
5	Organic nitrate chemistry and its implications for nitrogen budgets in an isoprene- and monoterpene-rich atmosphere: constraints from aircraft (SEAC <sup>4</sup> RS) and ground-based (SOAS) observations in the Southeast US. Atmospheric Chemistry and Physics. 2016. 16. 5969-5991.	4.9	173
6	Gridded National Inventory of U.S. Methane Emissions. Environmental Science & amp; Technology, 2016, 50, 13123-13133.	10.0	165
7	The role of chlorine in global tropospheric chemistry. Atmospheric Chemistry and Physics, 2019, 19, 3981-4003.	4.9	160
8	Quantifying methane emissions from the largest oil-producing basin in the United States from space. Science Advances, 2020, 6, eaaz5120.	10.3	155
9	Ozone pollution in the North China Plain spreading into the late-winter haze season. Proceedings of the United States of America, 2021, 118, .	7.1	138
10	Burden of Disease from Rising Coal-Fired Power Plant Emissions in Southeast Asia. Environmental Science & Technology, 2017, 51, 1467-1476.	10.0	122
11	An Ensemble Learning Approach for Estimating High Spatiotemporal Resolution of Ground-Level Ozone in the Contiguous United States. Environmental Science & Technology, 2020, 54, 11037-11047.	10.0	114
12	Global distribution of methane emissions, emission trends, and OH concentrations and trends inferred from an inversion of GOSAT satellite data for 2010–2015. Atmospheric Chemistry and Physics, 2019, 19, 7859-7881.	4.9	111
13	Observing atmospheric formaldehyde (HCHO) from space: validation and intercomparison of six retrievals from four satellites (OMI, GOME2A, GOME2B, OMPS) with SEAC <sup>4</sup> RS aircraft observations over the southeast US. Atmospheric Chemistry and Physics 2016, 16, 13477-13490	4.9	99
14	Atmospheric Chemistry and Physics 2016, 16 13477,13490 Using satellite observations of tropospheric NO <sub>2</sub> columns to infer long-term trends in US NO <sub><i>x</i></sub> emissions:Âthe importance of accounting for the free tropospheric NO <sub>2</sub>	4.9	89
15	background. Atmospheric Chemistry and Physics, 2019, 19, 8863-8878. Who Among the Elderly Is Most Vulnerable to Exposure to and Health Risks of Fine Particulate Matter From Wildfire Smoke?. American Journal of Epidemiology, 2017, 186, 730-735.	3.4	79
16	Global budget of tropospheric ozone: Evaluating recent model advances with satellite (OMI), aircraft (IAGOS), and ozonesonde observations. Atmospheric Environment, 2017, 167, 323-334.	4.1	74
17	Multidecadal trends in aerosol radiative forcing over the Arctic: Contribution of changes in anthropogenic aerosol to Arctic warming since 1980. Journal of Geophysical Research D: Atmospheres, 2017, 122, 3573-3594.	3.3	70
18	Attribution of the accelerating increase in atmospheric methane during 2010–2018 by inverse analysis of GOSAT observations. Atmospheric Chemistry and Physics, 2021, 21, 3643-3666.	4.9	68

#	Article	IF	CITATIONS
19	The 2005–2016 Trends of Formaldehyde Columns Over China Observed by Satellites: Increasing Anthropogenic Emissions of Volatile Organic Compounds and Decreasing Agricultural Fire Emissions. Geophysical Research Letters, 2019, 46, 4468-4475.	4.0	66
20	Satellite-based survey of extreme methane emissions in the Permian basin. Science Advances, 2021, 7, .	10.3	66
21	Global impact of nitrate photolysis in sea-salt aerosol on NO <sub><i>x</i></sub> , OH, and O <sub>3</sub> in the marine boundary layer. Atmospheric Chemistry and Physics. 2018. 18. 11185-11203.	4.9	62
22	Sensitivity to grid resolution in the ability of a chemical transport model to simulate observed oxidant chemistry under high-isoprene conditions. Atmospheric Chemistry and Physics, 2016, 16, 4369-4378.	4.9	60
23	A global gridded (0.1° × 0.1°) inventory of methane emissions from oil, gas, and coal exploitation ba on national reports to the United Nations Framework Convention on Climate Change. Earth System Science Data, 2020, 12, 563-575.	ased 9.9	60
24	Global methane budget and trend, 2010–2017: complementarity of inverse analyses using in situ (GLOBALVIEWplus CH <sub>4</sub> ObsPack) and satellite (GOSAT) observations. Atmospheric Chemistry and Physics, 2021, 21, 4637-4657.	4.9	55
25	Global distribution of methane emissions: a comparative inverse analysis of observations from the TROPOMI and GOSAT satellite instruments. Atmospheric Chemistry and Physics, 2021, 21, 14159-14175.	4.9	54
26	Unravelling a large methane emission discrepancy in Mexico using satellite observations. Remote Sensing of Environment, 2021, 260, 112461.	11.0	49
27	2010–2015 North American methane emissions, sectoral contributions, and trends: a high-resolution inversion of GOSAT observations of atmospheric methane. Atmospheric Chemistry and Physics, 2021, 21, 4339-4356.	4.9	45
28	High-resolution inversion of methane emissions in the Southeast US using SEAC <sup>4</sup> RS aircraft observations of atmospheric methane: anthropogenic and wetland sources. Atmospheric Chemistry and Physics, 2018, 18, 6483-6491.	4.9	38
29	Effect of sea salt aerosol on tropospheric bromine chemistry. Atmospheric Chemistry and Physics, 2019, 19, 6497-6507.	4.9	36
30	Monitoring global tropospheric OH concentrations using satellite observations of atmospheric methane. Atmospheric Chemistry and Physics, 2018, 18, 15959-15973.	4.9	34
31	Future respiratory hospital admissions from wildfire smoke under climate change in the Western US. Environmental Research Letters, 2016, 11, 124018.	5.2	29
32	Simulation of radon-222 with the GEOS-Chem global model: emissions, seasonality, and convective transport. Atmospheric Chemistry and Physics, 2021, 21, 1861-1887.	4.9	25
33	WRF-GC (v1.0): online coupling of WRF (v3.9.1.1) and GEOS-Chem (v12.2.1) for regional atmospheric chemistry modeling – Part 1: Description of the one-way model. Geoscientific Model Development, 2020, 13, 3241-3265.	3.6	25
34	Methane emissions in the United States, Canada, and Mexico: evaluation of national methane emission inventories and 2010–2017 sectoral trends by inverse analysis of in situ (GLOBALVIEWplus) Tj ETQq0 0 0 rgBT	/Qverlock 4.9	10 Tf 50 142
35	Atmospheric Chemistry and Physics, 2022, 22, 395-418. Enabling Highâ€Performance Cloud Computing for Earth Science Modeling on Over a Thousand Cores: Application to the GEOSâ€Chem Atmospheric Chemistry Model. Journal of Advances in Modeling Earth Systems, 2020, 12, e2020MS002064.	3.8	23
36	Harmonized Emissions Component (HEMCO) 3.0 as a versatile emissions component for atmospheric models: application in the GEOS-Chem, NASA GEOS, WRF-GC, CESM2, NOAA GEFS-Aerosol, and NOAA UFS models. Geoscientific Model Development, 2021, 14, 5487-5506.	3.6	23

#	Article	IF	CITATIONS
37	Updated Global Fuel Exploitation Inventory (GFEI) for methane emissions from the oil, gas, and coal sectors: evaluation with inversions of atmospheric methane observations. Atmospheric Chemistry and Physics, 2022, 22, 3235-3249.	4.9	22
38	Comparative analysis of low-Earth orbit (TROPOMI) and geostationary (GeoCARB, GEO-CAPE) satellite instruments for constraining methane emissions on fine regional scales: application to the Southeast US. Atmospheric Measurement Techniques, 2018, 11, 6379-6388.	3.1	17
39	WRF-GC (v2.0): online two-way coupling of WRF (v3.9.1.1) and GEOS-Chem (v12.7.2) for modeling regional atmospheric chemistry–meteorology interactions. Geoscientific Model Development, 2021, 14, 3741-3768.	3.6	17
40	Grid-independent high-resolution dust emissions (v1.0) for chemical transport models: application to GEOS-Chem (12.5.0). Geoscientific Model Development, 2021, 14, 4249-4260.	3.6	15
41	Enabling Immediate Access to Earth Science Models through Cloud Computing: Application to the GEOS-Chem Model. Bulletin of the American Meteorological Society, 2019, 100, 1943-1960.	3.3	14
42	GCAP 2.0: a global 3-D chemical-transport model framework for past, present, and future climate scenarios. Geoscientific Model Development, 2021, 14, 5789-5823.	3.6	11
43	Estimating 2010–2015 anthropogenic and natural methane emissions in Canada using ECCC surface and GOSAT satellite observations. Atmospheric Chemistry and Physics, 2021, 21, 18101-18121.	4.9	11
44	An Online‣earned Neural Network Chemical Solver for Stable Longâ€Term Global Simulations of Atmospheric Chemistry. Journal of Advances in Modeling Earth Systems, 2022, 14, .	3.8	10
45	Reduced-cost construction of Jacobian matrices for high-resolution inversions of satellite observations of atmospheric composition. Atmospheric Measurement Techniques, 2021, 14, 5521-5534.	3.1	5